HHS Public Access

Author manuscript

ACS Nano. Author manuscript; available in PMC 2016 April 28.

Published in final edited form as:

ACS Nano. 2015 April 28; 9(4): 3996–4005. doi:10.1021/nn507480v.

Identifying Sequential Substrate Binding at the Single-Molecule Level by Enzyme Mechanical Stabilization

Jaime Andrés Rivas-Pardo[‡,†,*], **Jorge Alegre-Cebollada**[‡], **César A. Ramírez-Sarmiento**[†], **Julio M. Fernandez**[‡,*], and **Victoria Guixé**[†,*]

[‡]Department of Biological Sciences, Columbia University, Northwest Corner Building, 550 West 120 Street, New York, New York 10027, USA

[†]Laboratorio de Bioquímica y Biología Molecular, Departamento de Biología, Facultad de Ciencias, Universidad de Chile, Las Palmeras 3425, Casilla 653, Santiago, Chile

Abstract

Enzyme-substrate binding is a dynamic process intimately coupled to protein structural changes, which in turn changes the unfolding energy landscape. By the use of single molecule force spectroscopy (SMFS), we characterize the open-to-closed conformational transition experienced by the hyperthermophilic ADP-dependent glucokinase from *Thermococcus litoralis* triggered by the sequential binding of substrates. In the absence of substrates, the mechanical unfolding of TlGK shows an intermediate I, which is stabilized in the presence of Mg·ADP$^-$, the first substrate to bind to the enzyme. However, in the presence of this substrate, an additional unfolding event is observed, intermediate-1*. Finally, in the presence of both substrates, the unfolding force of intermediates-1 and -1*, increases as a consequence of the domain closure. These results show that SMFS could be used as a powerful experimental tool to investigate binding mechanisms of different enzymes with more than one ligand, expanding the repertoire of protocols traditionally used in enzymology.

Keywords

single-molecule force spectroscopy; force-extension; mechanical intermediate; mechanical clamp; substrate stabilization

In recent years, evidence has accumulated demonstrating that the binding of substrates triggers a conformational rearrangement of enzyme structure.[1-4] In many cases, these conformational changes alternate through structural states that favor substrate binding, release of products, or protection of the transition state from attack by solvent molecules.[4-7]

[*]Address correspondence to jar2228@columbia.edu, jfernandez@columbia.edu or vguixe@uchile.cl.

Author Contributions: J.A.R-P., J.A-C., J.M.F. and V.G. designed the research project, J.A.R-P. performed the experiments, J.A.R-P., J.A-C. and J.M.F. analyzed the data. J.A.R-P., J.A-C., C.R-S., J.M.F. and V.G. co-wrote the paper.

Supporting Information Available: Histograms showing the unfolding forces of I27 module in the absence and presence of substrates is presented in Figure S1. Individual statistical error of the data collected for each condition, has been included in Table S1. Binding experiments, in the absence and presence of the substrates is presented in Figure S2. Additionally, possible locations of the mechanical intermediates and mechanical clamps present in ΔL_{C1} and ΔL_{C1*}, are shown in Figure S3 and S4. This material is available free of charge *via* the Internet at http://pubs.acs.org.

In addition, these conformational changes are related to the sequential binding of substrates.[2, 8-10] However, it is not easy to determine the presence of ligand binding, or the order in which binding occurs when more than one substrate is required. Since the seminal work of Cleland, determination of the kinetic mechanism of enzymes has been achieved using methods that involve enzyme activity assays in the presence of different concentrations of substrates, products and inhibitors.[11-15] Although this approach is well defined, in many cases there are practical barriers that prevent its realization, such as substrate inhibition, the absence of an appropriate coupled assay, and compound solubility, among others.[16-19] The mechanical stabilization of enzymes and proteins by ligand binding is a phenomenon that has been explored previously.[20-27] Substrates and ligands affect the energy landscape of different structural segments of a protein and in many cases increase the mechanical stability of the protein as a consequence of the favorable binding interactions.[28-30]

The ADP-dependent glucokinase from *Thermococcus litoralis* (TlGK) represents a suitable model to explore the mechanical stabilization of enzymes as a signature of the effective binding of substrates and inhibitors. TlGK exhibits sequential binding of its substrates, which correlates with well defined structural transitions that occur both in solution and in crystalline states.[31] TlGK is a hyperthermophilic enzyme that catalyzes the phosphate transfer from $Mg{\cdot}ADP^-$ to D-glucose, the first reaction of a modified version of the Embden-Meyerhof (EM) metabolic pathway present in archaea.[32] The structure of TlGK features a large Rossmann-like domain and a small α/β domain that emerges as a topological discontinuity,[33, 34] with the active site lying between both domains (Figure 1A). Substrate binding in TlGK has been proposed to follow a sequential ordered kinetic mechanism: $Mg{\cdot}ADP^-$ is the first substrate to bind to the enzyme, whereas D-glucose binds only when the $TlGK{\cdot}Mg{\cdot}ADP^-$ complex is already formed. Structural analysis reveals a conformational change from an open to a semi-closed state after nucleotide binding, while binding of D-glucose to this binary complex induces a fully-closed conformation (Figure 1A).[31]

Here we develop a single-molecule strategy to assess the sequential binding of substrates as an increase in the mechanical stability of TlGK, which is widely applicable to enzymes whose mechanical stability changes with the binding of substrates. Compared to more conventional methods, this strategy requires only a low concentration of enzyme, substrates, and inhibitors, and is independent of enzyme activity, which circumvents many of the problems associate with the traditional approaches employed in enzymology (kinetic assays) and provides a direct measurement of the protein-ligand interaction. As such it could be useful in drug design efforts since this strategy allows for the evaluation of the binding of inhibitors that modulate enzyme activity.

Results

Activity of TlGK in the polyprotein

In order to manipulate the protein at the single molecule level, TlGK was engineered into a polyprotein construct, with two I27 domains from human cardiac titin flanking both ends of the enzyme. The I27 domain from titin has been extensively studied, and its mechanical properties can be used as a “fingerprint” to identify unambiguously the manipulation of a

single molecule.[23, 35, 36] To confirm TlGK functionality in the $(I27)_2$-TlGK-$(I27)_2$ polyprotein, kinetic parameters for the phosphate transfer reaction were measured and compared with the values obtained for the soluble monomer. For both enzymes, saturation curves for $Mg{\cdot}ADP^-$ and D-glucose are very similar, yielding almost identical values for K_M and V_{max} (Figure 1B and Table 1). These results demonstrate that TlGK in the polyprotein construct is capable both of binding substrates and catalyzing phosphoryl transfer with unaltered kinetic constants.

Mechanical unfolding of Apo and Holo-enzyme

The polyprotein was pulled using a constant velocity protocol (400 $nm{\cdot}s^{-1}$). Figure 1C shows a characteristic force-extension trace corresponding to the unfolding of $(I27)_2$-TlGK-$(I27)_2$. We considered traces that show at least 3 unfolding events of the I27 module, in addition to the detachment event. The first unfolding event occurs at low force and after a large extension of the polyprotein (Figure 1C, arrow head), while the next events are essentially identical, since they share the same extension and force. These results indicate that the first mechanical event correspond to TlGK, mechanical intermediate-1, whereas the others belong to the unfolding of I27 modules.

For every trace recorded, four characteristic lengths were measured: full extension of the polypeptide (final extension, L_f), extension before I27 module unfolding (initial extension, L_i), extension of the mechanical intermediate present in TlGK and finally, extension of every I27 module (Figure 2A and Table 2). The average value for L_f is 314 ± 6 nm (Figure 2B), whereas the value for L_i is 193 ± 7 nm (Figure 2C). Assuming a length per residue of 0.4 nm,[37] the fully extended construct $(I27)_2$-TlGK-$(I27)_2$ should reach 339 nm (845 residues, see methods), whereas the extended TlGK + linkers (489 residues, see methods) should be 196 nm. Thus, our value for L_f and L_i are in very good agreement with the theoretical extension for the fully extended polyprotein and TlGK, respectively. The mechanical intermediate-1, which is present in the unfolding of TlGK, has an average extension of the contour length increment (ΔL_{CI}) of 61 ± 2 nm (Figure 2D), suggesting that ∼153 amino acids are involved in this mechanical intermediate. Finally, the contour length increment for I27 module ($\Delta L_{C\ I27}$) is 29 ± 1 nm (Figure 2E), in agreement with previously published values.[38, 39]

Thus, we measured the effect of the substrates on the mechanical unfolding of TlGK. The presence of the substrates produces no difference in the extension of L_i, L_f or ΔL_{C1} (Table 2). However, the substrates trigger an increase in the unfolding forces for the mechanical intermediate-1. We observed that this increase in the unfolding force is in accordance with the particular binding of the substrates. When the substrate $Mg{\cdot}ADP^-$ was assayed, the unfolding force increases from 43 ± 14 pN in the apo-enzyme to 54 ± 17 pN (Figure 3A and B, Table 3), whereas the unfolding force in the presence of D-glucose reaches only 47 ± 15 pN, which is not significantly different from the value obtained for the apo-enzyme (Figure 3A and C, Table 3). These results suggest that D-glucose does not bind to the enzyme in the absence of the $Mg{\cdot}ADP^-$, which is in agreement with previous kinetic experiments.[31] Finally, we explored the effect on the mechanical intermediate-1 when the ternary complex is mimicked by the use of the non-hydrolysable ADP analog, ADPβS. In the TlGK·

Mg·ADPβS-D-glucose complex, holo-enzyme, the unfolding force increased to 64 ± 15 pN (Figure 3A and D, Table 3), 20 pN more that the value observed in the apo-enzyme. Statistical analysis suggests that it is possible to identify three different mechanical states: (i) enzyme in the absence of substrate, apo-enzyme (E), (ii) enzyme in complex with $Mg{\cdot}ADP^-$ (E·A) and finally (iii) the enzyme with both substrates bound, holo-enzyme (E·A·B). All the unfolding forces are summarized in Table 3 and Table S1.

An additional mechanical intermediate was apparent in experiments where the enzyme was pulled as the E·A and E·A·B complexes (asterisk Figure 3 and Figure 4). This event is less populated in the apo-enzyme since we calculated that less than 20% of unfolding events visit this intermediate-1*. While, for the E·A and E·A·B conditions, 83% and 87% of the traces visit the intermediate-1*, respectively. In the E·A complex, the contour length for this intermediate, ΔL_{C1*}, is 68 ± 34 nm and the mechanical unfolding force is 52 ± 31 pN (Figure 4A and Table 4), whereas in the holo-enzyme the ΔL_{C1*} is 66 ± 22 nm and the unfolding force reaches a value of 93 ± 52 pN (Figure 4A and B, Table 4). The difference in force between these two conditions is statistically significant, therefore by using ΔL_{C1*} it is also possible to distinguish the E·A complex from the ternary E·A·B complex (Table 4 and Table S1).

Finally, to confirm the specificity of the stabilization effect achieved by substrates in TlGK, we used the unfolding forces of the I27 module as a control. As shown in Figure S1, the force necessary to unfold I27 remains close to ∼200 pN, regardless of the substrate present in the solution (Table 3 and Table S1). Thus, sequential binding of substrates is specific and affects only the unfolding forces of TlGK and not the I27 modules.

Inhibitors also change the mechanical stability of TlGK

Modulation of enzyme activity is a key aspect of proper cellular function. This can be achieved by inhibitory compounds that are structurally related to natural substrates but unable to support catalysis, or by allosteric effectors. In order to evaluate if mechanical stabilization is also exerted by TlGK inhibitors, we measured the mechanical stability of TlGK in the presence of $Mg{\cdot}GDP^-$, an analog of $Mg{\cdot}ADP^-$, and Mg·adenosine-5′-diphosphoglucose (Mg·ADP-GLC), which mimics ternary complex formation. In the presence of inhibitors we distinguish the same mechanical intermediate-1 and -1*, with no difference in the extension of ΔL_{C1} and ΔL_{C1*} (Table 2). However, both inhibitors trigger a mechanical stabilization of the mechanical intermediates. $Mg{\cdot}GDP^-$ increases the unfolding force for the intermediate-1 to 54 ± 15 pN, whereas Mg·ADP-GLC increases the unfolding force to 60 ± 18 pN, in good agreement with the values obtained for $Mg{\cdot}ADP^-$ binding (Figure 5, Table 3 and Table S1). These results in the presence of the inhibitors show statistical significant difference respect to the apo-enzyme, triggering a stabilization equivalent to the one detected in the presence of $Mg{\cdot}ADP^-$ (Table 4 and Table S1.). On the other hand, the mean value of the unfolding force for the mechanical intermediate-1* is 47 ± 16 pN in the presence of $Mg{\cdot}GDP^-$ and 49 ± 15 pN in the presence of Mg·ADP-GLC (Figure 5, Table 4 and Table S1.). In this case statistical analysis indicated that both inhibitors do not stabilize the intermediate-1* as occurs in E·A·B complex, rather the mechanical behavior is comparable to the binding of $Mg{\cdot}ADP^-$ (Table 4 and Table S1.).

Discussion

Determining the order of substrate binding in enzymes with more than one substrate is critical to understanding the individual steps involved in catalysis and is essential information for drug design. Traditional methods involve spectrophotometric techniques, which usually require large amounts of enzyme, substrates and inhibitors. Additionally, for many enzymes a direct method to detect product formation is not available, in which case, coupled-enzyme assays are extensively used. Also, there are several examples where is not possible to monitor the enzymatic activity in real time, requiring the use of complex and sophisticated techniques.[40, 41] In the case of TlGK, enzyme kinetic studies indicated a sequential ordered mechanism where $Mg{\cdot}ADP^-$ is the first substrate to bind to the enzyme (E·A complex), and D-glucose binds to the E·A complex, leading to ternary complex formation (E·A·B). These binding events are accompanied by successive conformational rearrangements. Small angle X-rays scattering studies indicate that the complex E·A closes slightly, and only after the binding of the D-glucose the domains closure is complete (Figure 1A).[31] Here we used mechanical perturbation of TlGK at the single molecule level to capture these different protein conformations. Force-extension experiments indicate the presence of two mechanical intermediates, ΔL_{C1} with an extension of 60 nm and ΔL_{C1*} with 66 nm, both sensitive to the binding of substrates (Table 2, 3 and 4). In the presence of both substrates (holo-enzyme), an additional 20 pN are needed to reach the unfolded state of the intermediate ΔL_{C1}. This change represents an increase of 50% in the force required to unfold the mechanical intermediate with respect to the apo-form. Furthermore, the intermediate-1* allows the clear distinction between complexes, with 44 pN of difference between E·A and E·A·B ternary complex. Additionally, the lack of change in the unfolding forces obtained in the presence of D-glucose suggests non-binding of the sugar in the absence of $Mg{\cdot}ADP^-$. However, binding without any change in the unfolding force has been reported before,[26] thus we cannot completely rule out this possibility. In the case of TlGK a sequential ordered kinetic mechanism has been proposed, where D-glucose is bound to the enzyme only after the complex $TlGK{\cdot}Mg{\cdot}ADP^-$ is formed.[31] Additionally, we have performed binding experiments that suggest that D-glucose binding occurs only in the presence of nucleotide (Figure S2). Thus the lack of change in force in the presence of D-glucose could be understood as the absence of D-glucose binding. Therefore, our results fully support the kinetic mechanism for the enzyme: binding of the $Mg{\cdot}ADP^-$ complex followed by the binding of D-glucose. In summary, our assay is able to detect at the single molecule level every state generated in solution during the catalytic reaction cycle (E, E·A and E·A·B).

During the last decades several models have emerged to explain the relationship between conformational changes and ligand binding. The *induced fit model*, originally raised by Koshland,[42] propose that the structure of the enzyme changes by the binding of ligands, whereas the *conformational selection model*, state that in solution the enzyme exist as an ensemble of conformations and only a fraction is able to bind ligands.[43, 44] Based on crystal structures, Sullivan and Holyoak demonstrate that the phosphoenolpyruvate carboxykinase operates through an induced fit mechanism, as well as other enzymes with lid-gated active sites.[7] For example, TlGK is α/β protein with two domains, where the small domains works

as lid on top of the active site (Figure S3).[34] If the enzyme reaches the closed conformation, there is not enough space for the substrates to access the active site, suggesting that conformational selection is not a plausible option. Our single molecule experiments are able to distinguish between apo- and holo-form (Figure 3 and 4), signatures of the open- and closed-conformations, respectively. These results could suggest that TlGK operates through an induced fit mechanism, where Mg·ADP$^-$ and D-glucose triggers the transition to the closed conformation. Prior work from our group based on crystal structures in the absence and presence of ligands and on the kinetic mechanism of TIGK, also pointed out the induced fit as the most probable mechanism.[31]

Additionally, our assay was also able to capture binding of inhibitors. TlGK·Mg·GDP$^-$ complex triggers a stabilization effect similar to the one observed in the presence of Mg·ADP$^-$, in agreement with the competitive inhibition exerted by the analog with respect to this substrate. On the other hand, the Mg·ADP-GLC ternary complex analog also exerts a mechanical stabilization, but in this case the stabilization is not equivalent to that found in the holo-enzyme; rather, it is similar to the effect observed in the presence of Mg·ADP$^-$ (Figure 5 and Table 4). It is probable that the different positions of the D-glucose hydroxyls in this analog impair the proper structural rearrangements related to catalysis in the enzyme. These results suggest that binding of Mg·GDP$^-$ or Mg·ADP-GLC precludes the formation of the E·A complex and induces conformational changes equivalent to the ones observed for the substrate Mg·ADP$^-$ although they are not able to sustain catalysis.

Mechanical stabilization by ligands at the single molecule level has been observed in other proteins. The force required to unfold the maltose binding protein can be modulated by the introduction of maltose in the solution,[20] which also has consequences on the unfolding pathway.[45] A similar effect was reported in titin kinase, where the introduction of ATP into the solution modifies the number of mechanical intermediates present in force-extension curves.[46] A very sophisticated example of mechanical unfolding modulation is observed in protein G and the Fc fragment of IgG.[47] Adding the Fc fragment at concentrations in the micromolar range increases the unfolding force from 100 pN to 200 pN. Furthermore, the change is concentration–dependent, thus it making possible to determine the dissociation constant for the IgG-Fc complex. However, to the best of our knowledge, TlGK is the first example of a sequential mechanical modulation, where protein stabilization follows the binding of substrates in accordance with the kinetic mechanism.

Moreover, TlGK unfolding follows a pathway with more than one intermediate that can be modified by the presence of substrates. In the apo-form, only 20% of the unfolding events present both mechanical intermediates. However, when Mg·ADP$^-$ or Mg·ADPβS·D-glc are added to the solution, more than 80% of the unfolding events show both mechanical intermediates. These results would suggest that binding of substrates modifies the unfolding pathway, from one to two mechanical intermediates. Examples of proteins with more than one mechanical intermediate have been described before. Leucine binding protein unfolds following a two-state pathway in the presence of leucine, but in the absence of substrate the unfolding become more complex and a multiple three-state pathway predominates.[30] Also, the phosphatidyl-*myo*-inositol mannosyltransferase A, shows a heterogeneous unfolding pathway with multiple steps.[48] In our case, TlGK is an enzyme of 467 residues with two

domains, which include several β-strands, thus the presence of multiple intermediates is highly probable. The mechanical intermediate-1, was present in all the conditions explored, whereas that the intermediate-1* was observed predominantly when substrates are bound to the enzyme, however highest stabilization is attained only in the E·A·B complex. Considering its fold and topology, several β-strands could be related to the mechanical clamp formation. Also, taking into account that the binding of both substrates change the mechanical stability of intermediate-1 and -1*, these should be in the neighborhood of the active site. Analysis of the holo-TlGK crystal structure reveals that the longest parallel β-structure present in the enzyme is located in the small domain between the β-strand 2 and 8 (residues Asn40 and Pro190) (Figure S3 and S4).[34] Therefore, considering that intermediate-1 should be located at the end of the unfolding pathway, capturing the last 60 nm of the protein -or 150 residues- (Table 2), the structure between β-strand 2 and β-strand 8 (150 residues) is a good candidate for the mechanical clamp present in the intermediate-1 (Figure S3B). On the other hand, assigning a specific structure to the mechanical intermediate-1*, which is reached when only a few amino acids are pulled from the enzyme, it is farther more complicated. Considering that both N- and C-terminus are located in the large domain of TlGK, is very likely that the mechanical clamp present in the intermediate-1* is formed by an arrangement of β-strands of this domain. A combination of parallel β-strands from the large domain, β-strands β1-β10-β11-β12-β13 (∼166 residues) can explain 66.4 nm (Figure S3C), very close to the extension of 66-68 nm observed in the ΔL_{C1*} (Table 4). However, if we consider that the full length of the enzyme is ∼190 nm (187 nm or 196 nm considering extension of likers, see methods), to reach intermediates-1 and -1* necessary a segment of the enzyme should be already unfolded. Approximately 70 nm of the enzyme should experience unfolding before intermediates-1 and 1*, which are not detecting during the mechanical unfolding with a distinguishable signature in force. The resting structure not considered in the intermediates-1 and 1*, includes α1 (residues 1 to 32) and the C-terminal α/β structure between β14 and α17 (residues 306 to 467) (Figure S2D). Both can explain around 77 nm (Figure S3D). It is known that antiparallel β-sheet and α-helix can be unfolded with less force than parallels β-sheet, with forces below 20 pN.[49] Therefore, is likely that α1 and α/β structure α17/β14 unfold at forces below our force limit, which is around 20-30 pN using this force-extension protocol.

Inspection in the crystal structures of TlGK reveals that both intermediates present residues involved in the stabilization of the substrates (Figure S4). Thus, it is possible to think that the binding of the complex $Mg{\cdot}ADP^-$ and D-glucose can be sensed by these intermediates. Additionally, α1 and α/β structure α17/β14 are not involved in the binding of D-glucose, and only Val440 (included in α17/β14 structure) whom participate in the binding of $Mg{\cdot}ADP^-$,[31] is removed during the mechanical unfolding. Therefore, the location of the substrate binding sites within the mechanical clamp explains the increase in mechanical stability of the intermediates when the unfolding is assayed in the presences of the substrates.

Conclusions

We have explored the strength of SMFS as a tool to assess the substrate-induced conformational changes experienced by the thermophilic enzyme TlGK in order to reach the

catalytic ternary complex. Our results not only provide information about the mechanical stabilization induced by the substrates on TlGK, but also embody the use of SMFS to identify its sequential order of binding to the active site. The combination of protein engineering and SMFS should be included among the techniques used to identify kinetic mechanism of enzymes or in the case of protein-protein and protein-ligand interactions. An SMFS-based approach is desirable because it requires very small amounts of enzyme and reagents, and multiple conditions can be explored easily, overcoming the drawbacks of traditional techniques. Additionally, our experimental assay can be applied to different systems and opens new alternatives to study protein-ligand interactions in solution, especially useful for the identification of modulators of enzyme activities with medical relevance, and for the discovery of new allosteric effectors. Besides, considering the new HaloTag technology for covalent anchoring,[50] which increases the pickup rate, fingerprint with full-length and the time that the molecule is attached to the surface/tip, the effect of the substrates and inhibitors in the unfolding and refolding of enzymes can be now studied in the same molecule.

Methods

Purification of the polyprotein $(I27)_2$-TlGK-$(I27)_2$

The TlGK polyprotein was engineered using the same strategy reported previously.[35] The cDNA coding for TlGK was kindly provided by Dr. Takayoshi Wakagi (University of Tokyo). Restriction sites *BamHI*, *BglII* and *KpnI* were added flanking the construct following a method described elsewhere.[38] The TlGK gene normally has a *BglII* restriction site that was removed and replaced by a silent mutation using GeneTailor site directed mutagenesis (Invitrogen). The final construct $(I27)_2$-TlGK-$(I27)_2$ was cloned into the expression vector pQE80L (Qiagen), by using the *BamHI* and *KpnI* restriction sites.

The full-length polyprotein comprises 847 amino-acid residues corresponding to four copies of I27 (89 residues each repeat), one copy of TlGK (467 residues), 13 extra amino acids in the N-terminus including a His-Tag, 2 residues in the C-terminus, and 2 residues between each module except between the TlGK and the next C-terminal I27 module, where the linker is composed of 3 residues (9 linker residues in total).

The polyprotein was expressed in *E. coli* BLR (DE3) pLysS cells at 25 °C. When the OD_{600nm} of the culture reached 0.7, protein expression was induced by 1 mM IPTG overnight. The cells were lysed by sonication and French press in sodium phosphate pH 7.0, 300 mM NaCl. The soluble fraction was loaded onto a Talon affinity chromatography column (Clontech). The fractions containing the polyprotein were pooled and run on a Superdex-200 size exclusion chromatography column (GE Healthcare), eluting with 10 mM Hepes pH 7.2, 150 mM NaCl, 1 mM EDTA. The fractions were analyzed by SDS-PAGE to ensure a homogeneous purification.

Enzyme kinetic experiments

We followed the activity of the TlGK by monitoring spectrophotometrically NAD^+ reduction at 340 nm coupled with the oxidation of D-glucose-6-phosphate. The enzyme

activity assays were carried out as described previously.[31] Briefly, each measurement was performed in 1 mL buffer with 25 mM Hepes pH 7.8, 0.5 mM NAD^+, 1 mM free Mg^{2+} and 5 units of D-glucose-6-phosphate deshydrogenase. For the $Mg{\cdot}ADP^-$ and D-glucose saturation curves the concentration of the co-substrate was fixed to 1 mM. Kinetics parameters, maximal velocity (V_{max}) and the apparent Michaelis constants for both substrates (K_M) were calculated by fitting initial velocities to the Michaelis-Menten model:

$$\nu_0 = \frac{\nu_{\max} \times S}{K_M + S} \quad \text{Equation 1}$$

Single molecule force spectroscopy

The experiments were performed using a custom-built atomic force microscope (AFM),[51] following the procedure described in Popa *et al.*[39] with a few modifications. Briefly, 5-10 μL of polyprotein sample from a ~0.1 $mg{\cdot}mL^{-1}$ stock solution was left to adsorb on a gold-coated glass coverslip. The fluid cell, mounted on top of the AFM, was sealed after 10-15 min of incubation to prevent full evaporation of the sample. MLCT cantilevers (Bruker) were calibrated using the equipartition theorem.[52] For our experiments the spring constants were between 14 and 20 $pN{\cdot}nm^{-1}$. In the force-extension experiments, a pulling velocity of 400 $nm{\cdot}s^{-1}$ was used. Single-molecule tethers were formed by pushing the cantilever against the polyprotein-containing surface for 0.5-1.0 s. All the measurements were made in 10 mM Hepes pH 7.2, 150 mM NaCl. For assays in the presence of both substrates 10 mM D-glucose, 7 mM Mg^{2+} and 5 mM ADPβS^{3-} (a non-hydrolysable analog of ADP^{3-}) were added. For experiments in the presence of only $Mg{\cdot}ADP^-$, 7 mM Mg^{2+} and 5 mM ADP^{3-} were added, whereas for only D-glucose assays, 10 mM D-glucose was added to the solution. For the experiments in the presence of the inhibitor $Mg{\cdot}GDP^-$, 11 mM Mg^{2+} and 10 mM GDP^{3-} was used. The molecule adenosine-5′-diphosphoglucose (ADP-GLC^{2-}), which has the nucleotide and sugar joined *via* a 5′ glycosidic linkage, was used as an analog to the ternary complex E·A·B. For this, 10 mM of adenosine-5′-diphosphoglucose (ADP-GLC^{2-}) supplemented with 11 mM Mg^{2+} were used. All the experiments were done at room temperature.

Data analysis

Only traces with at least three events of I27 unfolding were considered for analysis, this was to ensure that traces analyzed include the full unfolding of the enzyme TlGK. We used the elasticity polymer model Worm-Like Chain (WLC) to calculate the extension of the unfolding events.[53, 54] From the peak of these unfolding events we calculate the unfolding force for I27 and TlGK. We fitted Gaussian distribution to the unfolding extensions and unfolding forces histograms. The forces experienced for the mechanical intermediates present in TlGK (ΔL_{C1} and ΔL_{C1*}) and in I27 modules ($\Delta L_{C\ I27}$), were analyzed using one-way ANOVA considering individual unfolding force events. Bonferroni post-test was used to determine the significant differences between the pairs compared. The populations were considered significantly different when $P<0.05$.

Supplementary Material

Refer to Web version on PubMed Central for supplementary material.

Acknowledgments

This work was supported by Fondo Nacional de Desarrollo Científico y Tecnológico FONDECYT (grant 1110137 to V.G.). J.A.R-P. and C.A.R-S. were recipients of a doctoral fellowship from Comisión Nacional de Investigación Científica y Tecnológica (CONICYT). J.A.R-P. was receipt of visiting scholarship from the Becas Chile program. J.A-C. was supported by grant 1K99AI06072 from the National Institute of Health. J.M.F. is supported by National Institute of Health (grant HL61228) and National Science Foundation (grant 1252857). We thank Alejandra Herrera-Morande for the enzymatic activity controls in the presence of inhibitors. We also thank all members of the Fernandez laboratory for their helpful discussions.

References and Notes

1. Bakan A, Bahar I. The Intrinsic Dynamics of Enzymes Plays a Dominant Role in Determining the Structural Changes Induced Upon Inhibitor Binding. Proc Natl Acad Sci U S A. 2009; 106:14349–14354. [PubMed: 19706521]
2. Sigrell JA, Cameron AD, Mowbray SL. Induced Fit on Sugar Binding Activates Ribokinase. J Mol Biol. 1999; 290:1009–1018. [PubMed: 10438599]
3. Street TO, Lavery LA, Agard DA. Substrate Binding Drives Large-Scale Conformational Changes in the Hsp90 Molecular Chaperone. Mol Cell. 2011; 42:96–105. [PubMed: 21474071]
4. Zerrad L, Merli A, Schroder GF, Varga A, Graczer E, Pernot P, Round A, Vas M, Bowler MW. A Spring-Loaded Release Mechanism Regulates Domain Movement and Catalysis in Phosphoglycerate Kinase. J Biol Chem. 2011; 286:14040–14048. [PubMed: 21349853]
5. Cabrera R, Fischer H, Trapani S, Craievich AF, Garratt RC, Guixe V, Babul J. Domain Motions and Quaternary Packing of Phosphofructokinase-2 from Escherichia Coli Studied by Small Angle X-Ray Scattering and Homology Modeling. J Biol Chem. 2003; 278:12913–12919. [PubMed: 12527754]
6. Davulcu O, Flynn PF, Chapman MS, Skalicky JJ. Intrinsic Domain and Loop Dynamics Commensurate with Catalytic Turnover in an Induced-Fit Enzyme. Structure. 2009; 17:1356–1367. [PubMed: 19836335]
7. Sullivan SM, Holyoak T. Enzymes with Lid-Gated Active Sites Must Operate by an Induced Fit Mechanism Instead of Conformational Selection. Proc Natl Acad Sci U S A. 2008; 105:13829–13834. [PubMed: 18772387]
8. Tsuge H, Sakuraba H, Kobe T, Kujime A, Katunuma N, Ohshima T. Crystal Structure of the Adp-Dependent Glucokinase from Pyrococcus Horikoshii at 2.0-a Resolution: A Large Conformational Change in Adp-Dependent Glucokinase. Protein Sci. 2002; 11:2456–2463. [PubMed: 12237466]
9. Qasba PK, Ramakrishnan B, Boeggeman E. Substrate-Induced Conformational Changes in Glycosyltransferases. Trends Biochem Sci. 2005; 30:53–62. [PubMed: 15653326]
10. Ito S, Fushinobu S, Jeong JJ, Yoshioka I, Koga S, Shoun H, Wakagi T. Crystal Structure of an ADP-Dependent Glucokinase from Pyrococcus Furiosus: Implications for a Sugar-Induced Conformational Change in ADP-Dependent Kinase. J Mol Biol. 2003; 331:871–883. [PubMed: 12909015]
11. Cleland WW. The Kinetics of Enzyme-Catalyzed Reactions with Two or More Substrates or Products. I. Nomenclature and Rate Equations. Biochim Biophys Acta. 1963; 67:104–137. [PubMed: 14021667]
12. Cleland WW. The Kinetics of Enzyme-Catalyzed Reactions with Two or More Substrates or Products. II. Inhibition: Nomenclature and Theory. Biochim Biophys Acta. 1963; 67:173–187. [PubMed: 14021668]
13. Cleland WW. The Kinetics of Enzyme-Catalyzed Reactions with Two or More Substrates or Products. III. Prediction of Initial Velocity and Inhibition Patterns by Inspection. Biochim Biophys Acta. 1963; 67:188–196. [PubMed: 14021669]

14. Segel, IH. Enzyme Kinetics: Behavior and Analysis of Rapid Equilibrium and Steady State Enzyme Systems. Wiley Classics Library. , editor. Wiley; New York: 1993. p. 560-590.
15. Cleland, WW. Steady State Kinetics. In: Boyer, PD., editor. The Enzymes. 3. Academic Press; New York: 1970. p. 1-65.
16. Cleland WW. Substrate Inhibition. Methods Enzymol. 1979; 63:500–513. [PubMed: 502868]
17. McClure WR. A Kinetic Analysis of Coupled Enzyme Assays. Biochemistry. 1969; 8:2782–2786. [PubMed: 4241273]
18. Storer AC, Cornish-Bowden A. The Kinetics of Coupled Enzyme Reactions. Applications to the Assay of Glucokinase, with Glucose 6-Phosphate Dehydrogenase as Coupling Enzyme. Biochem J. 1974; 141:205–209. [PubMed: 4375970]
19. Cornish-Bowden, A. Fundamentals of Enzyme Kinetics. 3rd. Portland Press; London: 2004. p. 71-90.
20. Bertz M, Rief M. Ligand Binding Mechanics of Maltose Binding Protein. J Mol Biol. 2009; 393:1097–1105. [PubMed: 19733183]
21. del Rio A, Perez-Jimenez R, Liu R, Roca-Cusachs P, Fernandez JM, Sheetz MP. Stretching Single Talin Rod Molecules Activates Vinculin Binding. Science. 2009; 323:638–641. [PubMed: 19179532]
22. Kawamura S, Gerstung M, Colozo AT, Helenius J, Maeda A, Beerenwinkel N, Park PS, Muller DJ. Kinetic, Energetic, and Mechanical Differences between Dark-State Rhodopsin and Opsin. Structure. 2013; 21:426–437. [PubMed: 23434406]
23. Ainavarapu SR, Li L, Badilla CL, Fernandez JM. Ligand Binding Modulates the Mechanical Stability of Dihydrofolate Reductase. Biophys J. 2005; 89:3337–3344. [PubMed: 16100277]
24. Junker JP, Ziegler F, Rief M. Ligand-Dependent Equilibrium Fluctuations of Single Calmodulin Molecules. Science. 2009; 323:633–637. [PubMed: 19179531]
25. Wang CC, Tsong TY, Hsu YH, Marszalek PE. Inhibitor Binding Increases the Mechanical Stability of Staphylococcal Nuclease. Biophys J. 2011; 100:1094–1099. [PubMed: 21320455]
26. Junker JP, Hell K, Schlierf M, Neupert W, Rief M. Influence of Substrate Binding on the Mechanical Stability of Mouse Dihydrofolate Reductase. Biophys J. 2005; 89:L46–48. [PubMed: 16183885]
27. Cao Y, Yoo T, Li H. Single Molecule Force Spectroscopy Reveals Engineered Metal Chelation Is a General Approach to Enhance Mechanical Stability of Proteins. Proc Natl Acad Sci U S A. 2008; 105:11152–11157. [PubMed: 18685107]
28. Muller DJ. AFM: A Nanotool in Membrane Biology. Biochemistry. 2008; 47:7986–7998. [PubMed: 18616288]
29. Puchner EM, Gaub HE. Force and Function: Probing Proteins with AFM-Based Force Spectroscopy. Curr Opin Struct Biol. 2009; 19:605–614. [PubMed: 19822417]
30. Kotamarthi HC, Sharma R, Narayan S, Ray S, Ainavarapu SR. Multiple Unfolding Pathways of Leucine Binding Protein (Lbp) Probed by Single-Molecule Force Spectroscopy (Smfs). J Am Chem Soc. 2013; 135:14768–14774. [PubMed: 24015877]
31. Rivas-Pardo JA, Herrera-Morande A, Castro-Fernandez V, Fernandez FJ, Vega MC, Guixe V. Crystal Structure, Saxs and Kinetic Mechanism of Hyperthermophilic Adp-Dependent Glucokinase from Thermococcus Litoralis Reveal a Conserved Mechanism for Catalysis. PLoS One. 2013; 8:e66687. [PubMed: 23818958]
32. Sakuraba H, Goda S, Ohshima T. Unique Sugar Metabolism and Novel Enzymes of Hyperthermophilic Archaea. Chem Rec. 2004; 3:281–287. [PubMed: 14762828]
33. Wetlaufer DB. Nucleation, Rapid Folding, and Globular Intrachain Regions in Proteins. Proc Natl Acad Sci U S A. 1973; 70:697–701. [PubMed: 4351801]
34. Ito S, Fushinobu S, Yoshioka I, Koga S, Matsuzawa H, Wakagi T. Structural Basis for the Adp-Specificity of a Novel Glucokinase from a Hyperthermophilic Archaeon. Structure. 2001; 9:205–214. [PubMed: 11286887]
35. Perez-Jimenez R, Garcia-Manyes S, Ainavarapu SR, Fernandez JM. Mechanical Unfolding Pathways of the Enhanced Yellow Fluorescent Protein Revealed by Single Molecule Force Spectroscopy. J Biol Chem. 2006; 281:40010–40014. [PubMed: 17082195]

36. Alegre-Cebollada J, Badilla CL, Fernandez JM. Isopeptide Bonds Block the Mechanical Extension of Pili in Pathogenic Streptococcus Pyogenes. J Biol Chem. 2010; 285:11235–11242. [PubMed: 20139067]
37. Ainavarapu SR, Brujic J, Huang HH, Wiita AP, Lu H, Li L, Walther KA, Carrion-Vazquez M, Li H, Fernandez JM. Contour Length and Refolding Rate of a Small Protein Controlled by Engineered Disulfide Bonds. Biophys J. 2007; 92:225–233. [PubMed: 17028145]
38. Carrion-Vazquez M, Oberhauser AF, Fowler SB, Marszalek PE, Broedel SE, Clarke J, Fernandez JM. Mechanical and Chemical Unfolding of a Single Protein: A Comparison. Proc Natl Acad Sci U S A. 1999; 96:3694–3699. [PubMed: 10097099]
39. Popa I, Kosuri P, Alegre-Cebollada J, Garcia-Manyes S, Fernandez JM. Force Dependency of Biochemical Reactions Measured by Single-Molecule Force-Clamp Spectroscopy. Nat Protoc. 2013; 8:1261–1276. [PubMed: 23744288]
40. Holmgren A, Bjornstedt M. Thioredoxin and Thioredoxin Reductase. Methods Enzymol. 1995; 252:199–208. [PubMed: 7476354]
41. Kadokura H, Beckwith J. Mechanisms of Oxidative Protein Folding in the Bacterial Cell Envelope. Antioxid Redox Signal. 2010; 13:1231–1246. [PubMed: 20367276]
42. Koshland DE. Application of a Theory of Enzyme Specificity to Protein Synthesis. Proc Natl Acad Sci U S A. 1958; 44:98–104. [PubMed: 16590179]
43. Berger C, Weber-Bornhauser S, Eggenberger J, Hanes J, Pluckthun A, Bosshard HR. Antigen Recognition by Conformational Selection. FEBS Lett. 1999; 450:149–153. [PubMed: 10350075]
44. Kumar S, Ma B, Tsai CJ, Sinha N, Nussinov R. Folding and Binding Cascades: Dynamic Landscapes and Population Shifts. Protein Sci. 2000; 9:10–19. [PubMed: 10739242]
45. Aggarwal V, Kulothungan SR, Balamurali MM, Saranya SR, Varadarajan R, Ainavarapu SR. Ligand-Modulated Parallel Mechanical Unfolding Pathways of Maltose-Binding Proteins. J Biol Chem. 2011; 286:28056–28065. [PubMed: 21659518]
46. Puchner EM, Alexandrovich A, Kho AL, Hensen U, Schafer LV, Brandmeier B, Grater F, Grubmuller H, Gaub HE, Gautel M. Mechanoenzymatics of Titin Kinase. Proc Natl Acad Sci U S A. 2008; 105:13385–13390. [PubMed: 18765796]
47. Cao Y, Balamurali MM, Sharma D, Li HA. Functional Single-Molecule Binding Assay *via* Force Spectroscopy. Proc Natl Acad Sci U S A. 2007; 104:15677–15681. [PubMed: 17895384]
48. Giganti D, Alegre-Cebollada J, Urresti S, Albesa-Jove D, Rodrigo-Unzueta A, Comino N, Kachala M, Lopez-Fernandez S, Svergun DI, Fernandez JM, Guerin ME. Conformational Plasticity of the Essential Membrane-Associated Mannosyltransferase Pima from Mycobacteria. J Biol Chem. 2013; 288:29797–29808. [PubMed: 23963451]
49. West DK, Brockwell DJ, Olmsted PD, Radford SE, Paci E. Mechanical Resistance of Proteins Explained Using Simple Molecular Models. Biophys J. 2006; 90:287–297. [PubMed: 16214858]
50. Popa I, Berkovich R, Alegre-Cebollada J, Badilla CL, Rivas-Pardo JA, Taniguchi Y, Kawakami M, Fernandez JM. Nanomechanics of Halotag Tethers. J Am Chem Soc. 2013; 135:12762–12771. [PubMed: 23909704]
51. Oberhauser AF, Marszalek PE, Erickson HP, Fernandez JM. The Molecular Elasticity of the Extracellular Matrix Protein Tenascin. Nature. 1998; 393:181–185. [PubMed: 9603523]
52. Florin EL, Rief M, Lehmann H, Ludwig M, Dornmair C, Moy VT, Gaub HE. Sensing Specific Molecular-Interactions with the Atomic-Force Microscope. Biosensors & Bioelectronics. 1995; 10:895–901.
53. Marko JF, Siggia ED. Stretching DNA. Macromolecules. 1995; 28:8759–8770.
54. Rief M, Gautel M, Oesterhelt F, Fernandez JM, Gaub HE. Reversible Unfolding of Individual Titin Immunoglobulin Domains by AFM. Science. 1997; 276:1109–1112. [PubMed: 9148804]

Abbreviations

ADP	adenine diphosphate
AFM	atomic force microscope

SMFS	single molecule force spectroscopy
TlGK	ADP-dependent glucokinase from *Thermococcus litoralis*
WLC	worm-like chain

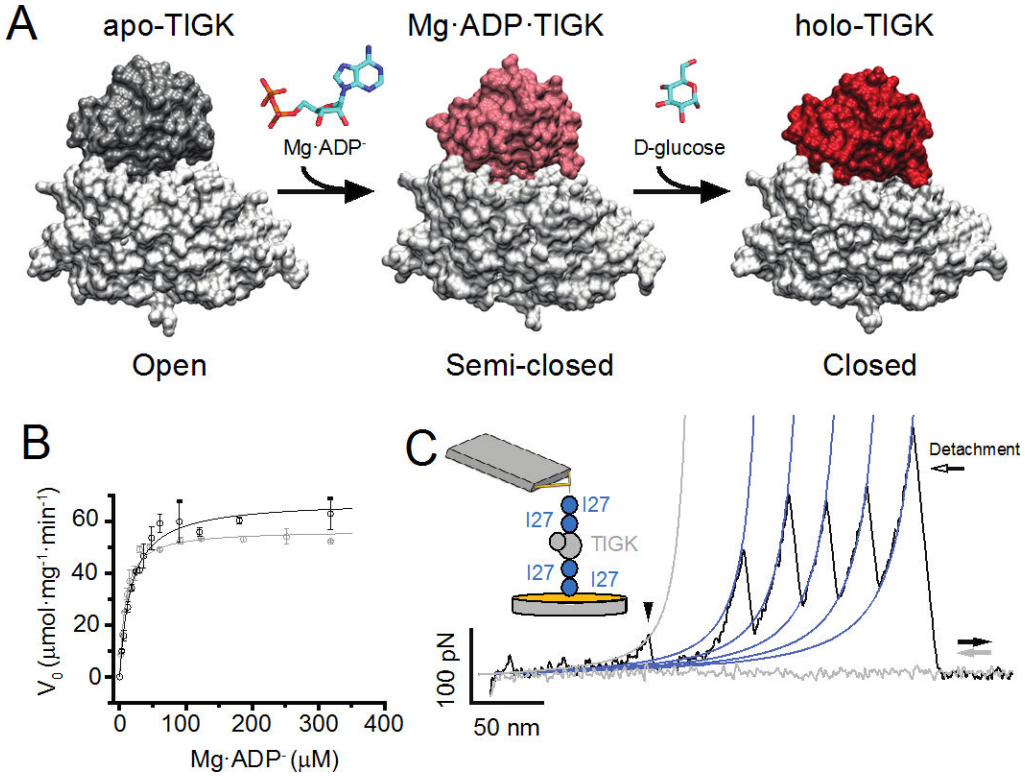

Figure 1. Single-molecule force spectroscopy of TlGK

(A) Crystal structures of TlGK. Substrate binding leads to conformational rearrangements, triggering the closure of domains. The large domain is colored in light gray for all conditions, whereas the small domains are shown in gray in the absence of substrate, pink in the presence of Mg·ADP$^-$, and red in the presence of both substrates. The binding site is located in the cleft formed between both domains. (B) Activity of the enzyme TlGK in the polyprotein. Mg·ADP$^-$ saturation curves for soluble monomer TlGK (gray circles) and $(I27)_2$-TlGK-$(I27)_2$ (black circles). Both curves were fitted using the Michaelis-Menten model (Equation 1). Table 1 summarizes the kinetic constant for the phosphate transfer reaction. (C) Representative trace for the mechanical unfolding of $(I27)_2$-TlGK-$(I27)_2$. Inset, shows a schematic representation of the polyprotein under mechanical tension. I27 modules are represented in blue, and TlGK in gray. The arrowhead indicates the main mechanical intermediate present in TlGK. Four consecutive peaks are detected, belonging to the unfolding of the I27 modules. The last peak at the end of each trace corresponds to the detachment of the protein from the cantilever or the gold surface. Fits correspond to the WLC model.[53, 54]

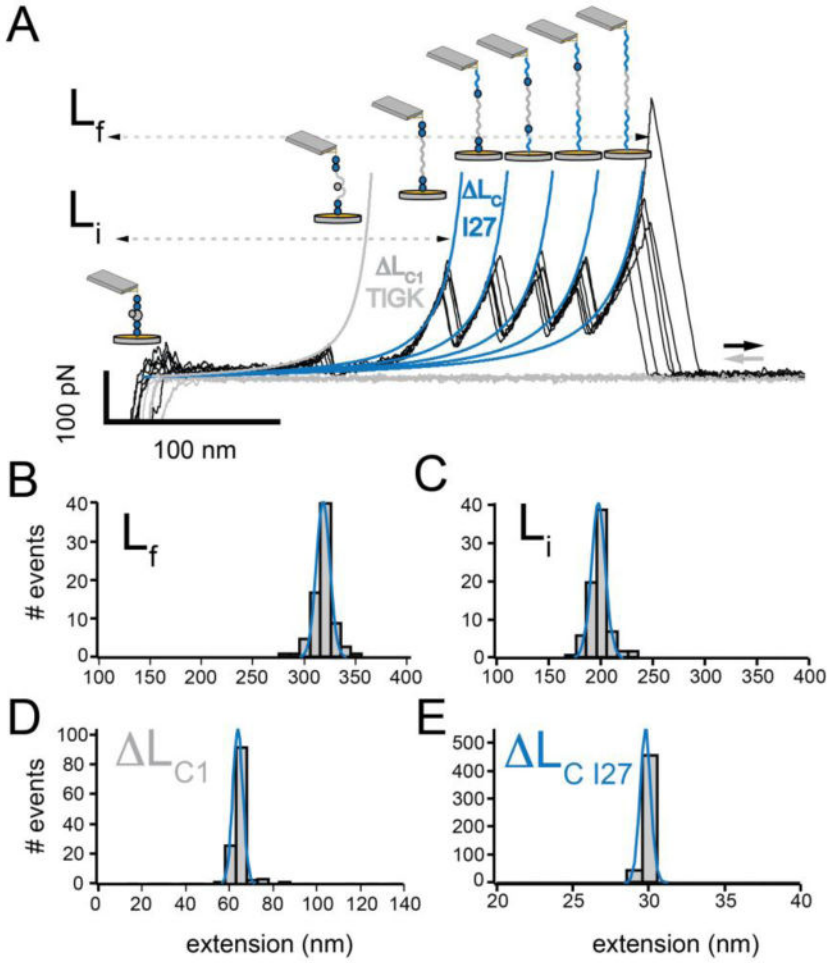

Figure 2. Fingerprint of the polyprotein $(I27)_2$-TIGK-$(I27)_2$

(A) Total lengths measured in the force-extension traces. Final extension (L_f) and initial extension of the polyprotein (L_i), correspond to the length where the polyprotein is totally unfolded and the extension of the polyprotein before the mechanical unfolding of the I27 modules, respectively. Fits correspond to the WLC model [53, 54]. (B) and (C) correspond to histograms of L_f and L_i, respectively. For L_f and L_i, only traces with four I27 events were considered (n=77). (D) and (E) contour length increment for the mechanical intermediate present in the TIGK (n=139) and I27 (511), respectively. Table 2 summarizes all the extensions calculated for the polyprotein.

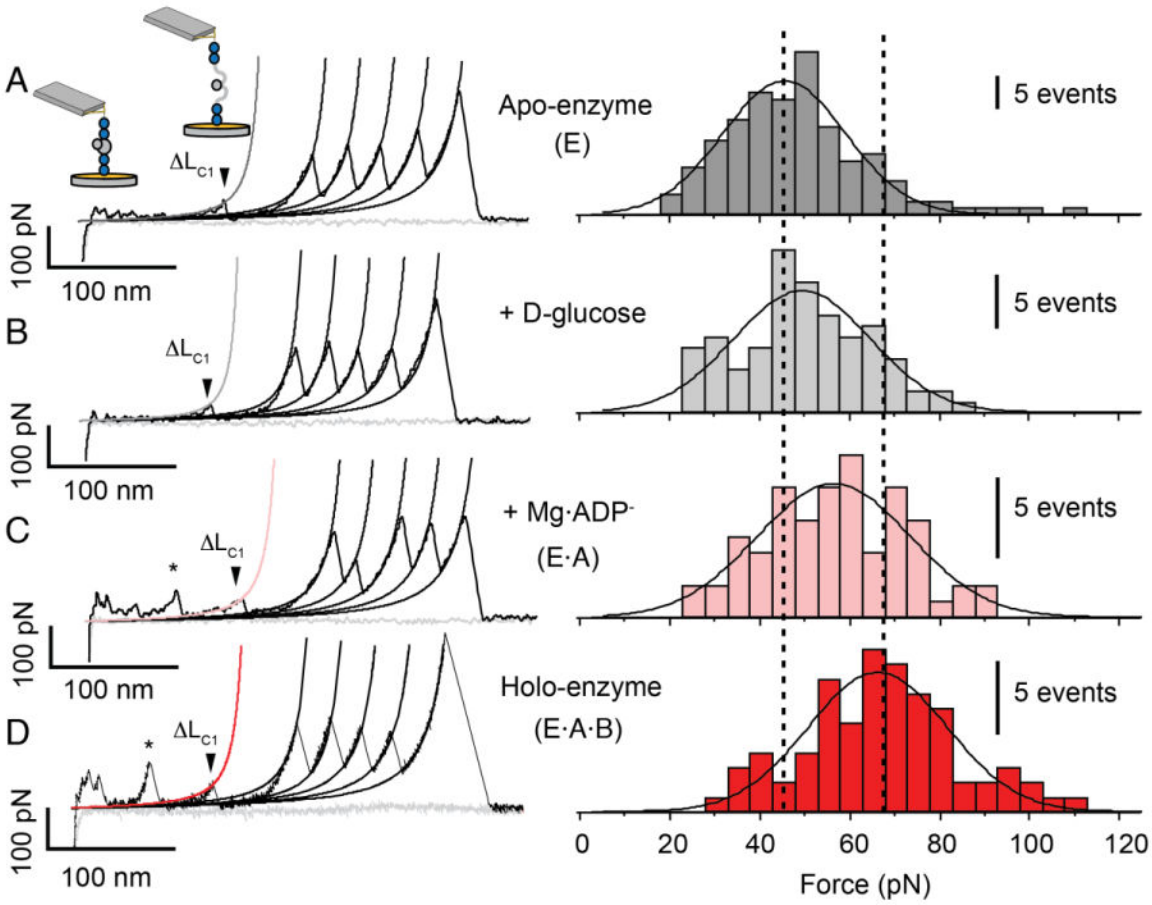

Figure 3. Mechanical stabilization of intermediate 1

(A-D) left, examples of force-extension traces under the different conditions explored: absence of substrates, presence of D-glucose, Mg·ADP$^-$ and holo-enzyme, respectively. Arrowhead shows the mechanical intermediate present in the TlGK. Note that traces in C and D shows an extra mechanical intermediate (asterisks). Fits in the traces correspond to the WLC model.[53, 54] The fits are shown in gray, light gray, pink and red, in accordance with the experimental condition. (A-D) right, histograms of the unfolding forces for ΔL_{C1}, under the same conditions. Bar shows the number of events. Solid black line corresponds to a Gaussian fit to the different conditions: apo-enzyme, D-glucose, Mg·ADP$^-$ and holo-enzyme. Dotted black lines indicate the transition for the unfolding force value between the apo and holo-enzyme. Table 3 and Table S1 summarize the unfolding forces for every experimental condition.

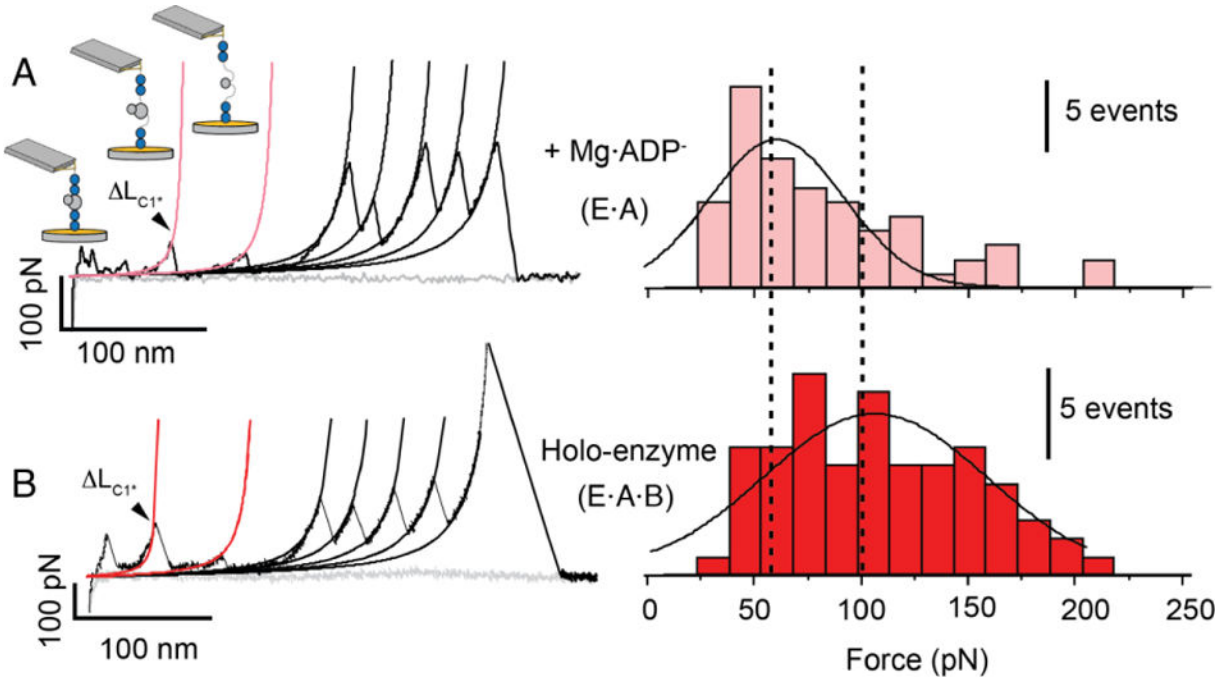

Figure 4. Mechanical intermediate 1* in the E·A and E·A·B complex

(A-B) left, force-extension traces of the unfolding in the presence of only Mg·ADP$^-$ and of both substrates, showing the additional mechanical intermediate 1* (arrowheads). Fits in the traces correspond to the WLC model.[53, 54] (A-B) right, histograms of the unfolding forces for ΔL_{C1*}, in the presence of Mg·ADP$^-$ and holo-enzyme. Bar shows the number of events. Solid black line corresponds to a Gaussian fit. Dotted black lines indicate the transition of the unfolding force value between the apo and holo-enzyme. The unfolding forces and extension for ΔL_{C1*} are summarized in Table 4 and Table S1.

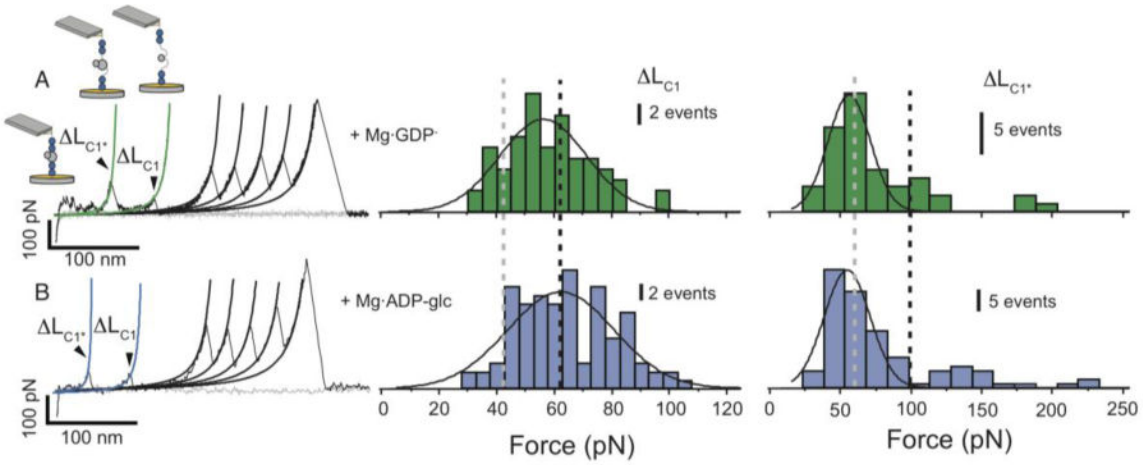

Figure 5. Mechanical stabilization by inhibitors of TlGK

(A-B) left, force-extension traces of the unfolding in the presence of $Mg{\cdot}GDP^-$ and Mg·ADP-GLC showing the both mechanical intermediates ΔL_{C1} and ΔL_{C1*} (arrowheads). Fits in the traces correspond to the WLC model.[53, 54] (A-B) middle and right, histograms of the unfolding forces for ΔL_{C1} and ΔL_{C1*}, respectively. Bars in the histograms correspond to the number of events. The unfolding forces and extension for the mechanical intermediates ΔL_{C1} and ΔL_{C1*} are summarized in Table 4 and Table S1.

Table 1
Enzyme kinetic parameters for ADP-dependent TlGK

	TlGK		$(I27)_2$-TlGK-$(I27)_2$	
	K_M (μM)	V_{MAX} ‡ (μmol·mg^{-1}·min^{-1})	K_M (μM)	V_{MAX} ‡ (μmol·mg^{-1}·min^{-1})
Mg·ADP$^-$	8.4 ± 0.7	57 ± 1	16 ± 2	67 ± 2
D-glucose	219 ± 2	57 ± 1	300 ± 5	67 ± 2

Values obtained from fitting the data to the Michaelis-Menten model (Equation 1). Values are given as mean ± standard deviation of the fit from three independent measurements. V_{MAX}‡ corresponds to the average value between measurements with Mg·ADP$^-$ and D-glucose as variable substrate.

Table 2

Mean extensions for the unfolding of $(I27)_2$-TlGK-$(I27)_2$

	L_f (nm)	L_i (nm)	I27 ΔL_{C1} (nm)	TlGK ΔL_{C1} (nm)	TlGK pL (nm)	n
Apo-enzyme	314 ± 6	193 ± 7	29.3 ± 0.4	61 ± 2	0.58 ± 0.11	139 (77)
D-glucose	304 ± 6	181 ± 8	29.0 ± 0.5	59 ± 3	0.54 ± 0.17	88 (51)
Mg·ADP$^-$	328 ± 14	207± 16	29.5 ± 0.4	61 ± 3	0.48 ± 0.18	71 (41)
Holo-enzyme	315 ± 8	195 ± 8	29.7 ± 0.5	62 ± 4	0.44 ± 0.13	82 (50)
Mg·GDP$^-$	323 ± 15	196 ± 13	29.6 ± 0.5	59 ± 3	0.46 ± 0.12	64 (48)
Mg·ADP-GLC	309 ± 14	186 ± 6	29.36 ± 0. 03	60 ± 4	0.43 ± 0.11	107 (77)

Distances were calculated using the WLC model.[53, 54] L_f and L_i consider only traces with four I27 unfolding events. pL is the persistence length fitted from the WLC model. n corresponds to the total number of unfolding events. The numbers in parenthesis correspond to traces with four I27 unfolding events used for L_f and L_i. The extension values reported correspond to the mean value ± standard deviation from Gaussian fits (Figure 2).

Table 3

Mean unfolding forces of ΔL_{C1} and $\Delta L_{C\ I27}$

	TlGK			I27		
	Force (pN)	**n**	**(*P*)**	**Force (pN)**	**n**	**(*P*)**
Apo-enzyme	43 ± 14	139	-	213 ± 24	511	-
D-glucose	47 ± 15	88	>0.05	214 ± 29	315	>0.05
Mg·ADP$^-$	54 ± 17	71	<0.05	215 ± 24	259	>0.05
Holo-enzyme	64 ± 15	82	<0.001	213 ± 23	297	>0.05
Mg·GDP$^-$	54 ± 15	64	<0.05	212 ± 23	238	>0.05
Mg·ADP-GLC	60 ± 18	107	<0.001	227 ± 26	401	>0.05

The forces reported in the table are the mean value ± standard deviation from the Gaussian fits (Figure 3). Statistical analysis was made using one-way Anova. *P* values in the table are considering apo-conditon as reference.

Table 4

Mean extensions and unfolding forces of ΔL_{C1*}

	Extension (nm)	pL (nm)	Force (pN)	(*P*)	n	%
Holo-enzyme	66 ± 22	0.5 ± 0.2	93 ± 52	-	72	87
Mg·ADP$^-$	68 ± 34	0.5 ± 0.2	53 ± 31	<0.01	59	83
Mg·GDP$^-$	68 ± 9	0.57 ± 0.09	47 ± 16	<0.001	44	69
Mg·ADP-GLC	67 ± 21	0.4 ± 0.1	49 ± 15	<0.001	92	86

The forces reported in the table are the mean value ± standard deviation from the Gaussian fits (Figure 4 and 5). pL is the persistence length fitted from the WLC model.[53, 54] Statistical analysis was made using one-way Anova. *P* values in the table are considering Holo-enzyme as reference.